

Expediting Feller process with stochastic resetting

Somrita Ray*

Department of Chemistry, Indian Institute of Technology Tirupati, Tirupati 517619, India

(Dated: July 27, 2022)

We explore the effect of stochastic resetting on the first-passage properties of Feller process. The Feller process can be envisioned as space-dependent diffusion, with diffusion coefficient $D(x) = x$, in a potential $U(x) = x(\frac{x}{2} - \theta)$ that owns a minimum at θ . This restricts the process to the positive side of the origin and therefore, Feller diffusion can successfully model a vast array of phenomena in biological and social sciences, where realization of negative values is forbidden. In our analytically tractable model system, a particle that undergoes Feller diffusion is subject to Poissonian resetting, i.e., taken back to its initial position at a constant rate r , after random time epochs. We addressed the two distinct cases that arise when the relative position of the absorbing boundary (x_a) with respect to the initial position of the particle (x_0) differ, i.e., for (a) $x_0 < x_a$ and (b) $x_a < x_0$. Utilizing the Fokker-Planck description of the system, we obtained closed-form expressions for the Laplace transform of the survival probability and hence derived the exact expressions of the mean first-passage time $\langle T_r \rangle$. Performing a comprehensive analysis on the optimal resetting rate (r^*) that minimize $\langle T_r \rangle$ and the maximal speedup that r^* renders, we identify the phase space where Poissonian resetting facilitates first-passage for Feller diffusion. We observe that for $x_0 < x_a$, resetting accelerates first-passage when $\theta < \theta_c$, where θ_c is a critical value of θ that decreases when x_a is moved away from the origin. In stark contrast, for $x_a < x_0$, resetting accelerates first-passage when $\theta > \theta_c$, where θ_c is a critical value of θ that increases when x_0 is moved away from the origin. Our study opens up the possibility of a series of subsequent works with more case-specific models of Feller diffusion with resetting.

I. INTRODUCTION

The Feller process is a special kind of Markovian random process with a linear drift term and a state-dependent diffusion term, which vanishes at the origin[1–4]. Such specific choices of the drift and diffusion terms ensure that the process is always restricted to the positive side of the origin. In other words, realization of negative values is absolutely forbidden for Feller diffusion, which in turn makes it a suitable model for describing a number of phenomena that are relevant in biological and social sciences. For example, the Feller process is frequently used as an alternative to the well-known Lotka-Volterra model[5, 6] to describe the time evolution of the population of a species in a locality, since it (Feller diffusion) includes the effect of fluctuating environment[7–9]. One focal point of interest in these problems is to investigate the possibilities of extinction of that species and/or the unrestricted growth of its population, which can be extracted from the first-passage[10] properties of the Feller process. The Feller neuronal model[11–16] is a simple yet effective one to recount the firing of single neurons. This integrate and fire model describes the fluctuations in membrane potential that regulates the nerve impulses; as this potential crosses a threshold value, the neuronal activity happens due to the firing of an action potential (nerve impulse), which lowers the membrane potential to some previous value and the cycle repeats. The firing dynamics can thus be explored by studying the associated first-passage properties of the Feller model[11–16].

Feller diffusion finds wide applications in the financial markets as well. For example, the well-celebrated CIR (Cox, Ingersoll and Ross) model[17] is nothing but a Feller process that describes the temporal evolution of interest rate, where

the randomness is originated solely from the market risk factor. Feller diffusion is also utilized for incorporating randomness in the volatility of asset prices[18–20], the latter being a statistical measure of the dispersion of the returns from those assets[21]. For these reasons and others, Feller process has received a steady attention for the last few decades in biophysics and economics.

While Feller diffusion serves as a classic model to the cases mentioned above, there are quite a few situations where the original problem of Feller diffusion is not sufficient to explain the dynamics. For example, epidemics and natural disasters can abruptly diminish the population of a species in a geographic location, thereby setting it back to an earlier value[22]. In a similar way, during financial market crashes, the stock prices may drastically reduce to a prior asset value[23]. In these cases, Feller diffusion with *stochastic resetting* should serve as an excellent model.

Stochastic resetting[24–27] implies a situation where an ongoing dynamical process is stopped at random intervals of time, usually by some external protocol, to start over. Resetting can either shorten or prolong the completion of a stochastic process depending on the physical governing parameters. Tuning such parameters, it is (in principle) possible to invert such effect of resetting on the dynamics[28–35]. Due to its appearance in a plethora of natural systems and drastic effect on the dynamics, study of first-passage problems with resetting has gained overwhelming attention in recent years[36–51]. Surprisingly, the effect of resetting on Feller process still remains scarcely explored. To bridge this gap, in this paper we present a comprehensive analysis on the first-passage properties of Feller diffusion with resetting.

The rest of this paper is organized as follows. In Sec. II we discuss the equation of motion for the Feller process to visualize it as diffusion in a potential and revisit some earlier results associated to the first-passage properties of Feller diffusion

* somrita@iittp.ac.in

without resetting. In the same Section, with the aid of the theory of first-passage with resetting[28, 29], we predict when resetting is expected to accelerate first-passage for Feller diffusion. In Sec. III, we start with the Fokker Planck description of Feller diffusion with Poissonian resetting and obtain a general expression of the survival probability in the Laplace space, which depends on the boundary conditions. Considering that the target value is higher than the initial value of the associated first-passage process, in Sec. IV we first derive an exact, closed-form expression of the survival probability in the Laplace space, and then explore the phase space where resetting expedites Feller process. In Sec. V we repeat the entire study for the case where the target value is lower than the initial value of the Feller process. The final conclusions are drawn in Sec. VI.

II. THE FELLER PROCESS

The Feller process[1–4] is a special kind of Markovian random process with a linear deterministic force term (drift term) and a multiplicative noise term (diffusion term). Letting $X(t)$ denote a Feller process, its equation of motion can be written as

$$dX(t) = a[b - X(t)]dt + \sigma\sqrt{X(t)}dW(t), \quad (1)$$

where $a, b, \sigma > 0$ are constant parameters and $W(t)$ is a Wiener process[52], which represents the integral of a Gaussian white noise. Eq. (1) shows that the process has a linear drift term, $f(X, t) := a[b - X(t)]$, and a space-dependent diffusion term $D(X, t) := \sigma^2 X(t)$. Therefore, for $X(t) = 0$, the drift term becomes $f(0, t) = ab > 0$ (i.e., at the origin, the drift is directed towards its positive side) and the diffusion term becomes $D(0, t) = 0$. These indicate that the Feller process $X(t)$ is always restricted to the positive side of the origin.

To simplify Eq. (1) further, we scale time as $t' \rightarrow at$ and the process as $x \rightarrow (2a/\sigma^2)X$ to rewrite Eq. (1) as

$$\frac{dx(t')}{dt'} = \theta - x(t') + \sqrt{2x(t')}\eta(t'), \quad (2)$$

where $\theta \equiv 2ab/\sigma^2 > 0$ is the sole, constant and dimensionless governing parameter for the scaled process, which gives the rate of change of $x(t')$ at the origin, i.e., $\theta = [dx(t')/dt']_{x \rightarrow 0}$. In Eq. (2), $\eta(t') := dW(t')/dt'$ denotes a Gaussian white noise given by $\langle \eta(t') \rangle = 0$ and $\langle \eta(t')\eta(t'') \rangle = \delta(t' - t'')$. This scaled description of the Feller diffusion will be considered throughout this paper. To avoid unnecessary complexity in the notation, we shall drop the prime and simply use t to denote the scaled time variable from now on. Next, we briefly discuss how Feller process can be realized as inhomogeneous diffusion in a non-linear/non-monotonic potential.

A. Feller process as diffusion in a potential

Eq. (2) clearly indicates that the scaled process is analogous to space-dependent diffusion of a Brownian particle with diffusion coefficient $D(x) = x$ in a force-field $-U'(x) = (\theta - x)$

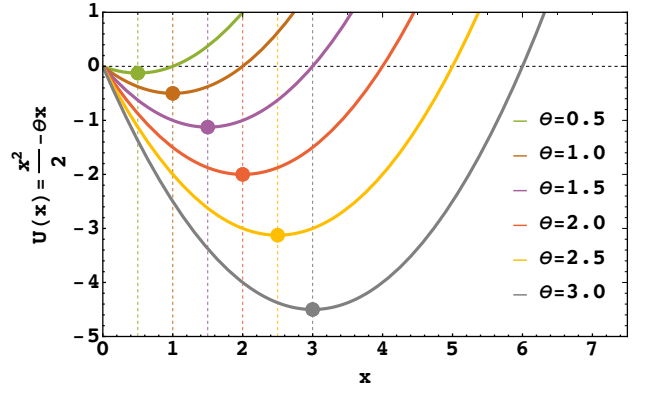


FIG. 1. Feller process, as described in Eq. (2), can be envisioned as diffusion in a potential $U(x) = x(\frac{x}{2} - \theta)$. As θ increases, the potential gradually becomes deeper and its minimum, which lies at θ , shifts toward right.

that vanishes at $x = \theta$ [also evident from Eq. (3)], where x is the dimensionless position of that diffusing particle. This force-field is generated from a potential $U(x) = x(\frac{x}{2} - \theta)$. Taking a more engaging look at the shape of $U(x)$, we see that it is a unique harmonic potential, where the equilibrium or minimum position lies at θ . With increase in θ , the potential becomes deeper and its minimum moves towards right [see Fig. 1]. Note that the inhomogeneous diffusion invokes some asymmetry in this otherwise symmetric potential $U(x)$. Since the diffusion at the origin is zero and it increases linearly with x , the effective potential that the particle experiences at the left side of $x = \theta$, the stable point of the potential, is always stronger compared to that at the right side of it. These features of Feller diffusion make the problem a rather complicated one to analyse, and we expect non-trivial outcomes in the first-passage properties. Indeed, depending on the relative placements of the initial position of the particle (denoted x_0) and the placement of the absorbing boundary (until which the first-passage is considered, denoted x_a) with respect to θ , the Feller diffusion of interest can be either uphill or downhill (or a combination of both). Therefore, the relative placements of θ , x_0 and x_a will dictate whether the interplay between the drift velocity, generated from the potential, and the inhomogeneous diffusion will assist or oppose the first-passage to x_a . We will discuss this aspect in greater details later, while analysing the conditions where resetting facilitates first-passage. Now, we focus on constructing the Fokker-Planck equation associated to Feller diffusion in order to extract the first-passage properties.

B. Fokker-Planck equation and survival probability

The Fokker-Planck equation[24, 52] associated to Eq. (2) reads

$$\frac{\partial}{\partial t} p(x, t|x_0) = \frac{\partial}{\partial x} [(x - \theta)p(x, t|x_0)] + \frac{\partial^2}{\partial x^2} [xp(x, t|x_0)], \quad (3)$$

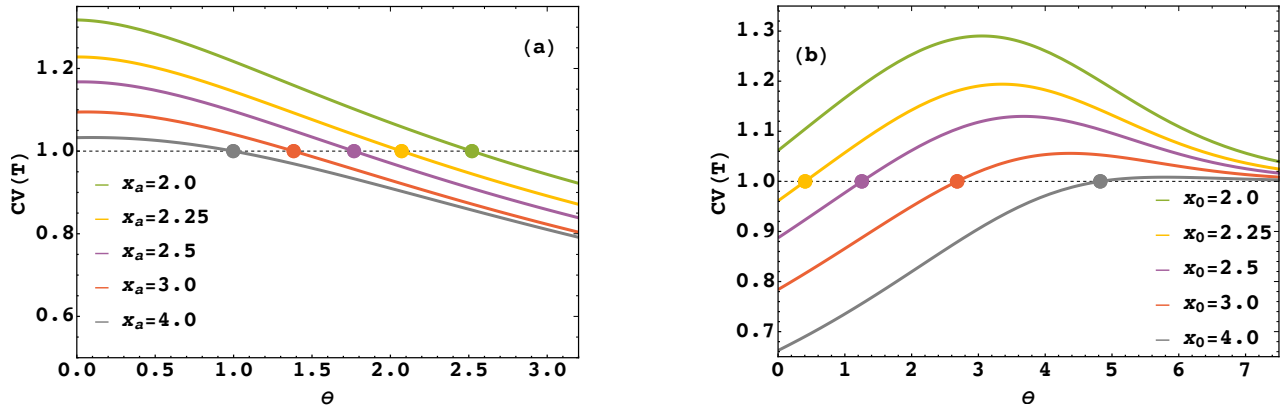


FIG. 2. Panel(a): The coefficient of variation $CV(T)$ in the FPT vs. θ [following Eq. (A.30) from Appendix A] for different values of x_a , keeping x_0 constant, where $x_0 < x_a$ in all cases. $CV(T)$ is greater than unity for lower values of θ , indicating that resetting should expedite first-passage from the initial position x_0 to the absorbing boundary at x_a in that regime. Panel(b): The coefficient of variation $CV(T)$ in the FPT vs. θ [following Eq. (A.35) from Appendix A] for different values of x_0 , keeping x_a constant, where $x_a < x_0$ in all cases. In contrast to the previous case, $CV(T)$ is greater than unity for higher values of θ , which indicates that resetting should expedite first-passage from x_0 to x_a in that regime.

where $p(x, t|x_0)$ is the conditional probability density function for the process to be at position x at time t , the initial condition being $p(x, 0|x_0) = \delta(x - x_0)$. Since $0 < x < \infty$ represent the natural boundaries for Feller diffusion, the initial condition uniquely specifies p . From Eq. (3), we can write the backward Fokker-Planck equation[24, 53] in terms of the survival probability, i.e., the total probability density that the process survives within an interval Ω at time t , $Q(t|x_0) := \int_{\Omega} p(x, t|x_0) dx$, which reads

$$\frac{\partial}{\partial t} Q(t|x_0) = (\theta - x_0) \frac{\partial}{\partial x_0} Q(t|x_0) + x_0 \frac{\partial^2}{\partial x_0^2} Q(t|x_0). \quad (4)$$

Recently, the first-passage properties of a Feller process have been explored[2], where it was shown that the first-passage to a threshold value x_a that is above the initial value x_0 , the survival probability in the Laplace space is given by

$$\tilde{Q}(s|x_0) = \frac{1}{s} \left[1 - \frac{M(s; \theta; x_0)}{M(s; \theta; x_a)} \right], \quad (5)$$

where $\tilde{Q}(s|x_0) := \int_0^{\infty} e^{-st} Q(t|x_0) dt$ denotes the Laplace transform of $Q(t|x_0)$, where s is the Laplace variable. $M(s; \theta; y)$ in Eq. (6) is the confluent hypergeometric function of the first kind[54], defined as

$$M(s; \theta; y) := \sum_k \frac{\Gamma(s+k)}{\Gamma(\theta+k)} \frac{y^k}{k!}, \quad (6)$$

where $\Gamma(c) := \int_0^{\infty} t^{c-1} e^{-t} dt$ is the *gamma function*. It has also been established that when the threshold value x_a lies below the initial value x_0 , the survival probability in the Laplace space is given by

$$\tilde{Q}(s|x_0) = \frac{1}{s} \left[1 - \frac{U(s; \theta; x_0)}{U(s; \theta; x_a)} \right], \quad (7)$$

where $U(s; \theta; y)$ is the confluent hypergeometric function of the second kind[54], expressed in terms of $M(s; \theta; y)$ as

$$U(s; \theta; y) := \pi \csc(\pi\theta) \left[-y^{1-\theta} \frac{M(s-\theta+1; 2-\theta; y)}{\Gamma(s)} + \frac{M(s; \theta; y)}{\Gamma(s-\theta+1)} \right]. \quad (8)$$

The survival probability contains complete information of the associated first-passage process. In particular, when a process takes a random time T to complete, the first and second moments of that time can be calculated from its survival probability in the Laplace space[53] as $\langle T \rangle = [\tilde{Q}(s|x_0)]_{s \rightarrow 0}$ and $\langle T^2 \rangle = -2 \left[\frac{d\tilde{Q}(s|x_0)}{ds} \right]_{s \rightarrow 0}$, respectively. Next, we briefly discuss how one can predict whether the introduction of stochastic resetting can reduce that mean time of completion or not, based on these two quantities.

C. Can stochastic resetting accelerate Feller diffusion?

Stochastic resetting, i.e., bringing a diffusing particle back to its initial position after random intervals of time, can either facilitate or hinder a first-passage process. The theory of first-passage with resetting[28, 29] states that resetting expedites a first-passage process whenever the standard deviation of the associated first-passage time (FPT), $\sigma(T) := [\langle T^2 \rangle - \langle T \rangle^2]^{\frac{1}{2}}$, is greater than the mean first-passage time, $\langle T \rangle$. In complete contrast, when $\sigma(T) < \langle T \rangle$, resetting delays first-passage. Since the coefficient of variation in FPT is defined as $CV(T) := \sigma(T) / \langle T \rangle$, one can alternatively say that whenever the $CV(T) > 1$, resetting reduces the mean FPT of the process, otherwise (i.e., when $CV(T) < 1$) the original process is hindered due to resetting and the associated mean FPT increases as a result. In physical systems, the mean FPT,

$\langle T \rangle$, and the fluctuations around it, quantified by $\sigma(T)$, both vary when the governing parameters are altered. This indicates that by tuning physical parameters, the effect of resetting on the dynamics can be inverted.

In order to get a qualitative idea about how resetting affects the first-passage for Feller diffusion, we calculate the associated $CV(T)$ for the following two conditions. First, utilizing Eq. (5) we calculate $CV(T)$ for $x_0 < x_a$ [see Appendix A for details], and plot the same in Fig. 2(a) with respect to θ for different values of x_a , keeping x_0 constant. Fig. 2(a) clearly shows that $CV(T) > 1$ for smaller values of θ , which indicates that resetting expedites first-passage there. When θ increases beyond a threshold value, however, $CV(T)$ decreases below unity, which means resetting delays first-passage in that regime. Next, utilizing Eq. (7) we calculate $CV(T)$ as a function of θ for $x_a < x_0$, for different values of x_0 keeping x_a constant [see Appendix A for details]. Plotting the same in Fig. 2(b), we observe that in stark contrast to the previous case, here resetting hinders first-passage for smaller values of θ and accelerates the same as θ grows beyond a critical value. These observations suggest that based on the governing parameters, viz., θ , x_a and x_0 , resetting can either expedite or delay first-passage for Feller process. While this condition based on $CV(T)$ gives a general idea about the regimes where resetting facilitates (or hinders) first-passage, it fails to comment on the quantitative aspect of the resulting speedup (or delay). Nonetheless, it suggests that Feller diffusion can lead to non-trivial first-passage properties when subject to resetting. Motivated by these initial findings, we now perform a comprehensive analysis on the effect of Poissonian resetting on the dynamics of Feller diffusion.

III. FELLER PROCESS WITH RESETTING

Consider a particle executing Feller diffusion in one dimension following Eq. (1), starting from a position $x_0 > 0$. In addition, assume that by some external protocol, it is being stochastically reset to a position $x_r > 0$ at a constant rate r . This means that the random times between two subsequent resetting events are chosen from an exponential distribution with mean r^{-1} . Consider an absorbing boundary placed at $x_a > 0$; when the particle hits it for the first time, it gets absorbed and the process is complete. Letting $p_r(x, t|x_0)$ denote the conditional probability density of finding the particle at position x at time t , provided its initial position was x_0 , we write down the forward Fokker Planck equation[24, 30, 33, 34] for the process as

$$\begin{aligned} \frac{\partial}{\partial t} p_r(x, t|x_0) = & \frac{\partial}{\partial x} [(x - \theta) p_r(x, t|x_0)] + \frac{\partial^2}{\partial x^2} [x p_r(x, t|x_0)] \\ & - r p_r(x, t|x_0) + r \delta(x - x_r) Q_r(t|x_0), \end{aligned} \quad (9)$$

where $Q_r(t|x_0) := \int_{\Omega} p_r(x, t|x_0) dx$ is the survival probability within the interval Ω (i.e., the total probability of finding the particle within Ω at time t). Note that the placement of the absorbing boundary with respect to the initial position dictates

the interval that the particle is within. For $x_0 < x_a$, $\Omega = [0, x_a]$ and for $x_a < x_0$, $\Omega = [x_a, \infty)$.

It is evident from Eq. (9) that in the absence of resetting, Eq. (9) boils down to Eq. (1), the Fokker Planck equation of the original Feller process. For $r > 0$, probability of being at position x decreases and that at x_r increases due to resetting, and the two additional terms appear in Eq. (9) to account for this additional probability flow.

The backward Fokker Planck equation in terms of the survival probability $Q_r(t|x_0)$ thus reads[24, 33, 34]

$$\begin{aligned} \frac{\partial}{\partial t} Q_r(t|x_0) = & (\theta - x_0) \frac{\partial}{\partial x_0} Q_r(t|x_0) + x_0 \frac{\partial^2}{\partial x_0^2} Q_r(t|x_0) \\ & - r Q_r(t|x_0) + r Q_r(t|x_r). \end{aligned} \quad (10)$$

Laplace transforming Eq. (10) and utilizing the initial condition, $Q_r(0|x_0) = 1$, we get

$$\begin{aligned} x_0 \frac{\partial^2}{\partial x_0^2} \tilde{Q}_r(s|x_0) + (\theta - x_0) \frac{\partial}{\partial x_0} \tilde{Q}_r(s|x_0) - (s + r) \tilde{Q}_r(s|x_0) \\ = -[1 + r \tilde{Q}_r(s|x_r)], \end{aligned} \quad (11)$$

where $\tilde{Q}_r(s|x_0) := \int_0^\infty e^{-st} Q_r(t|x_0) dt$ denotes the Laplace transform of $Q_r(t|x_0)$. To convert the non-homogeneous differential equation shown in Eq. (11) to a homogeneous one, consider a constant shift

$$\tilde{q}_r(s|x_0) = \tilde{Q}_r(s|x_0) - \frac{1 + r \tilde{Q}_r(s|x_r)}{s + r}. \quad (12)$$

This allows us to write down Eq. (11) in terms of $\tilde{q}_r(s|x_0)$ as

$$x_0 \frac{\partial^2}{\partial x_0^2} \tilde{q}_r(s|x_0) + (\theta - x_0) \frac{\partial}{\partial x_0} \tilde{q}_r(s|x_0) - (s + r) \tilde{q}_r(s|x_0) = 0. \quad (13)$$

Eq. (13) resembles Kummer's equation [55, 56], which is a confluent hypergeometric equation with general solution

$$\tilde{q}_r(s|x_0) = c_1 M(s + r; \theta; x_0) + c_2 U(s + r; \theta; x_0). \quad (14)$$

Here $M(s + r; \theta; x_0)$ and $U(s + r; \theta; x_0)$ are the confluent hypergeometric functions of the first and second kind[54], as introduced in Eq. (6) and Eq. (8), respectively. Combining Eq. (12) and Eq. (14) together, we can write down the general solution of Eq. (11) that reads

$$\begin{aligned} \tilde{Q}_r(s|x_0) = & c_1 M(s + r; \theta; x_0) + c_2 U(s + r; \theta; x_0) \\ & + \frac{1 + r \tilde{Q}_r(s|x_r)}{s + r}. \end{aligned} \quad (15)$$

To find out the specific solution of Eq. (11), we need to calculate c_1 and c_2 from the boundary conditions. The absorbing boundary at x_a leads to $\tilde{Q}_r(s|x_a) = 0$. However, the specific solutions of Eq. (11) will depend on the placement of x_a with respect to the initial position x_0 , as mentioned above. Once $\tilde{Q}_r(s|x_0)$ is calculated for the appropriate scenario, we can utilize that solution to calculate the

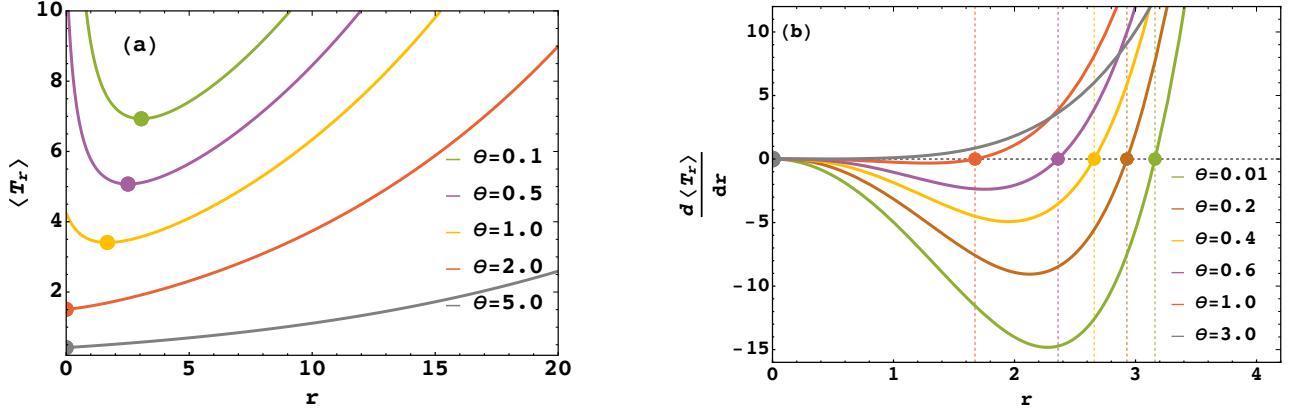


FIG. 3. First-passage with resetting for $x_0 < x_a$. Panel (a): The mean FPT $\langle T_r \rangle$ vs. the resetting rate r for different values of θ , where $x_0 = 1$ and $x_a = 2.5$. $\langle T_r \rangle$ shows non-monotonic variation with r for lower values of θ ; the optimal resetting rates (r^*), marked by colored discs, are non-zero in this regime. In contrast, for higher values of θ , the variation of $\langle T_r \rangle$ with r becomes monotonic and r^* become zero in this regime. Panel (b): Graphical solution of Eq. (19) for different values of θ , where $x_0 = 1$ and $x_a = 2.5$. The solutions that present the optimal resetting rate (r^*) in each case, are marked by colored discs.

first-passage time of the particle from x_0 to x_a , denoted T_r , in the following manner. Recall that the probability density of T_r is given by $-dQ_r(t|x_0)/dt$, which allows us to calculate the moments of T_r following the general relation[53]

$$\langle T_r^n \rangle = -\int_0^\infty t^n \left[\frac{dQ_r(t|x_0)}{dt} \right] dt \equiv n(-1)^{n-1} \left[\frac{d^{n-1} \tilde{Q}_r(s|x_0)}{ds^{n-1}} \right]_{s=0}.$$

In Section IV, we focus on the case $x_0 < x_a$, i.e., where the boundary is placed at the right hand side of the initial position, and explore the first-passage from the initial position x_0 to the boundary at x_a .

IV. FIRST-PASSAGE FROM x_0 TO x_a : WHEN THE ABSORBING BOUNDARY IS PLACED FURTHER AWAY FROM THE ORIGIN COMPARED TO THE INITIAL POSITION ($x_0 < x_a$)

Consider the case where $x_0 < x_a$, i.e., when the particle diffuses in the interval $\Omega = [0, x_a]$. Note that the placement of the boundary further away from the origin compared to the initial position suggests that in this case, the first-passage is being considered from a less diffusive to a more diffusive zone. Going back to Eq. (15), we see that in the limit $x_0 \rightarrow 0$, $U(s+r; \theta; x_0)$ diverges for $\theta > 1$. Hence we set $c_2 = 0$ to keep $\tilde{Q}_r(s|x_0)$ finite, irrespective of the values of θ . The absorbing boundary at x_a then leads to $c_1 = -[1 + r\tilde{Q}_r(s|x_r)] / [(s+r)M(s+r; \theta; x_a)]$. The specific solution of Eq. (11) for $x_0 < x_a$ thus becomes

$$\tilde{Q}_r(s|x_0) = \frac{1 + r\tilde{Q}_r(s|x_r)}{s+r} \left[1 - \frac{M(s+r; \theta; x_0)}{M(s+r; \theta; x_a)} \right]. \quad (16)$$

Setting $x_r = x_0$ in Eq. (16), i.e, equating the position of reset to the initial position, allows us to obtain an explicit expression of $\tilde{Q}_r(s|x_0)$, which reads

$$\tilde{Q}_r(s|x_0) = \frac{1 - \frac{M(s+r; \theta; x_0)}{M(s+r; \theta; x_a)}}{s+r \left[\frac{M(s+r; \theta; x_0)}{M(s+r; \theta; x_a)} \right]}. \quad (17)$$

Note that in the absence of resetting, i.e, when $r \rightarrow 0$, the survival probability in the Laplace space for $x_0 < x_a$ reduces to the expression given in Eq. (5).

The mean first-passage time from x_0 to an absorbing boundary at x_a can be obtained from Eq. (17) as $\langle T_r \rangle = [\tilde{Q}_r(s|x_0)]_{s=0}$, which gives

$$\langle T_r \rangle = \frac{1}{r} \left[\frac{M(r; \theta; x_a)}{M(r; \theta; x_0)} - 1 \right]. \quad (18)$$

In Fig. 3(a), we plot the mean FPT $\langle T_r \rangle$ vs. the resetting rate r following Eq. (18), keeping x_0 and x_a constant. Fig. 3(a) shows that for lower values of θ , $\langle T_r \rangle$ varies non-monotonically with r ; when r is small, $\langle T_r \rangle$ decreases as r grows, but for higher values of the resetting rate, the mean FPT increases with r . A minimum in mean FPT for an *optimal* resetting rate is thus observed. As θ increases beyond a critical value [denoted θ_c , not shown in Fig. 3(a)], however, the mean FPT monotonically increases with the resetting rate, which indicates that resetting can not expedite first-passage in that case. These two distinct types of variation of $\langle T_r \rangle$ with r show a hallmark of *resetting transition*[30–34]. Fig. 3(a) also shows that the optimal resetting rate, i.e, the resetting rate that corresponds to the minimum mean FPT, is zero when the variation of $\langle T_r \rangle$ with r is monotonic. When $\langle T_r \rangle$ shows non-monotonic variation with r , the optimal resetting rate increases as θ becomes smaller. This suggests that the optimal resetting rate, denoted r^* , should serve as an excellent observable in exploring the resetting transition for the present problem. Next, we calculate r^* as a function of θ to understand the resetting transition in greater depth.

A. The optimal resetting rate for $x_0 < x_a$

Since the optimal resetting rate minimizes the mean FPT, the rate of change of the mean FPT with the resetting rate becomes zero at $r = r^*$, i.e, $\left[\frac{d\langle T_r \rangle}{dr} \right]_{r=r^*} = 0$. Therefore, differ-

entiating Eq. (18) with respect to r and equating that to zero for $r = r^*$, we obtain

$$\left[\frac{d\langle T_r \rangle}{dr} \right]_{r=r^*} = \frac{1}{(r^*)^2 M(r^*; \theta; x_0)} \left[-r^* M(r^*; \theta; x_a) \left(\frac{\partial M(r; \theta; x_0)}{\partial r} \right)_{r=r^*} + M(r^*; \theta; x_0) [M(r^*; \theta; x_0) - M(r^*; \theta; x_a) + r^* \left[\frac{\partial M(r; \theta; x_a)}{\partial r} \right]_{r=r^*}] \right] = 0 \quad (19)$$

Eq. (19) is a transcendental equation, hence not solvable analytically. Fig. 3(b) shows its graphical solution, where the left hand side of Eq. (19) is plotted against r for different values of θ , and the points of intersection of each curve with the abscissa give the corresponding optimal resetting

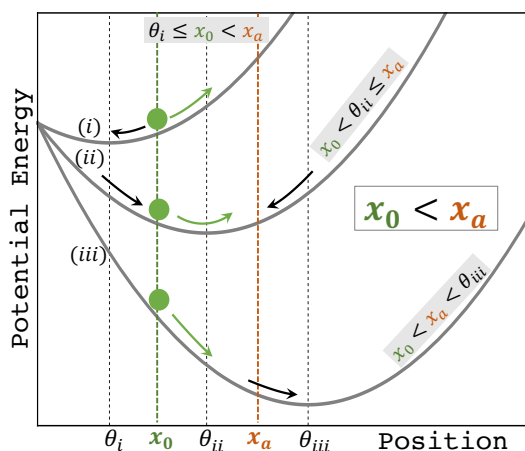


FIG. 4. Schematic plot of the potential $U(x) = x(\frac{x}{2} - \theta)$ vs. x to envision Feller process as space-dependent diffusion in $U(x)$. The three scenarios that arise in connection to the first-passage from x_0 to x_a , where $x_0 < x_a$, are illustrated with three $U(x)$ curves with different minima, such that $\theta_i < \theta_{ii} < \theta_{iii}$. The green arrow in each case indicates the overall direction of the first-passage, whereas the black arrows indicate the drift velocity generated by $U(x)$ in each case. When these two forces oppose each other [e.g., $\theta_i \leq x_0 < x_a$], resetting is expected to expedite first-passage. In contrast, when these forces assist each other [e.g., $x_0 < x_a < \theta_{iii}$], resetting is expected to delay first-passage. An intermediate case is observed for $x_0 < \theta_{ii} \leq x_a$.

rate. As observed from Fig. 3(b), the optimal resetting rates are higher for smaller values of θ , indicating that resetting accelerates the first-passage when $\theta < \theta_c$. As θ grows, r^* decreases and finally becomes zero for $\theta \geq \theta_c$, which means that there resetting can not expedite the first-passage. This trend can be qualitatively understood by considering Feller process as space-dependent diffusion, with diffusion coefficient $D(x) = x$, in a potential $U(x) = x(\frac{x}{2} - \theta)$, as discussed in Section II. If we focus on the relative placements of θ with x_0 and x_a , we see that three distinct possibilities arise: (i) $\theta \leq x_0 < x_a$, (ii) $x_0 < \theta \leq x_a$ and (iii) $x_0 < x_a < \theta$. In Fig. 4, we plot the potential energy $U(x)$ vs. the position x to illustrate these three cases. Recalling that the minimum of the potential $U(x)$ lies at θ , the first-passage for case (i) is clearly

an uphill journey [marked by the green arrow above curve (i)], whereas for case (iii) it is a downhill one [marked by the green arrow above curve (iii)]. In other words, for case (i) the drift velocity acts away from the absorbing boundary and thereby opposes the first-passage [marked by the black arrow above curve (i)]; resetting at $x_0 > \theta$ thus helps accelerating the process. In stark contrast, for case (iii) the drift velocity acts towards x_a [marked by the black arrow above curve (iii)] and thereby assists the first-passage; resetting at $x_0 < \theta$ thus interrupts the process and delays it. Case (ii) represents an intermediate scenario between these two extreme cases, shown by curve (ii) in Fig. 4.

To develop a deeper understanding of the transition observed in Fig. 3(a) and 3(b), we numerically solve Eq. (19) to calculate r^* as a function of θ for different values of x_a (keeping x_0 constant), and plot the same in Fig. 5. It is clear from Fig. 5 that when x_0 is kept constant, as the distance of the absorbing boundary from the origin (x_a) increases, the transition appears at lower values of θ_c . The three independent parameters, viz. x_0 , x_a and θ_c , make the dynamics quite complicated to analyse, nonetheless, we try to understand this trend qualitatively as follows. Recall that for Feller process, the diffusion is inhomogeneous in space; the movement of the particle close to the origin is almost deterministic and it

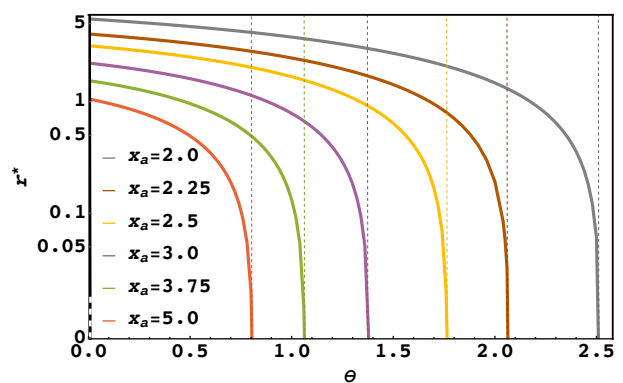


FIG. 5. The optimal resetting rate r^* vs. θ , obtained from the numerical solution of Eq. (19), for different positions of the absorbing boundary, x_a , when $x_0 < x_a$. The non-zero values of r^* , observed for lower values of θ , mark the regime when resetting accelerates first-passage from x_0 to x_a . The resetting transitions are indicated by the dashed vertical lines with the same color as the curves. The initial position is kept fixed at $x_0 = 1$ in each case. With increase in x_a , the transition is observed to take place at lower values of θ .

gradually becomes more and more diffusive when the particle moves away from the origin. In addition, the Feller potential owns a minimum at $x = \theta$. When the distance between x_0 and x_a is small and both are placed somewhat close to the *trapping zone* created by θ , resetting at x_0 can reduce the otherwise long time spent in that trapping zone and accelerate the first-passage by incorporating some directed motion towards x_a . Keeping x_0 and θ unaltered, if the absorbing boundary is moved away from the origin (which is equivalent to moving vertically downward at any certain θ in Fig. 5), the role of diffusion in the dynamics becomes more and more prominent. Thus, when the distance between x_0 and x_a is large, diffusion near the absorbing boundary is quite high. Resetting the particle to a position x_0 , where the dynamics is much less diffusive, clearly interrupts the first-passage as each resetting event makes the particle cross the trapping zone and travel the long distance between x_0 to x_a all over again. This explains why the optimal resetting rate gradually decreases with increase in x_a for any particular value of θ in Fig. 5. The trapping becomes more significant as θ increases [as the potential well becomes deeper, see Fig. 1] and that enhances the interruption that resetting triggers in case of longer travel distances. As a result, the resetting transition appears at lower θ_c as x_a is placed further away from the origin. In fact, when x_a is placed at a distance far enough, resetting at x_0 will only help if $\theta < x_0$, by successfully counteracting the trapping events at $x < x_0$. Summarizing, we see that for $x_0 < x_a$, resetting expedites first-passage for $\theta < \theta_c$ and θ_c decreases as the distance to travel increases. After analysing Fig. 5 in a qualitative manner, we proceed to calculate the maximal speedup to quantify the effect of optimal resetting on the dynamics.

B. Maximal speedup for $x_0 < x_a$

Resetting with an optimal rate renders the maximal speedup of a first-passage process. We define maximal speedup as the ratio between the mean FPT for the original process (i.e., the process without resetting) to the mean FPT of the process with optimal resetting, i.e. $\langle T \rangle / \langle T_{r^*} \rangle$. Setting $r = r^*$ in Eq. (18) and utilizing Eq. (A.28) from Appendix A [that gives the mean FPT of the original process], we can write down the following expression for the maximal speedup

$$\frac{\langle T \rangle}{\langle T_{r^*} \rangle} = \frac{r^* \left(\left[\frac{\partial M(s; \theta; x_a)}{\partial s} \right]_{s \rightarrow 0} - \left[\frac{\partial M(s; \theta; x_0)}{\partial s} \right]_{s \rightarrow 0} \right)}{\frac{M(r^*; \theta; x_a)}{M(r^*; \theta; x_0)} - 1}. \quad (20)$$

Plugging in r^* [that we calculated earlier by numerically solving Eq. (19)] into Eq. (20), we calculate the maximal speedup of the first-passage process from x_0 to x_a , when $x_0 < x_a$. Plotting Eq. (20) with respect to θ for different values of x_a in Fig. 6, we see that the maximal speedup is most significant when θ is small, indicating that resetting in this regime helps the most. With increase in θ , however, the maximal speedup gradually decreases, until it becomes unity

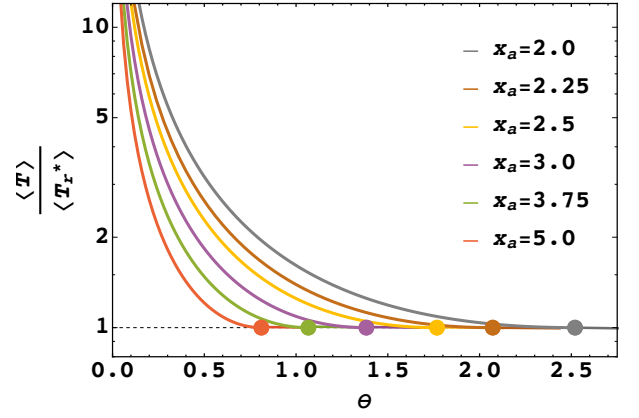


FIG. 6. Maximal speedup $\langle T \rangle / \langle T_{r^*} \rangle$ [due to resetting with an optimal rate r^*] vs. θ following Eq. (20) for different values of x_a , where $x_0 < x_a$. The colors of the curves correspond to the cases shown in Fig. 5. The most significant maximal speedup is observed for lower values of θ . With gradual increase of θ past a critical value, the resetting transition [marked by colored discs] takes place and the maximal speedup becomes unity thereafter, which indicates that resetting no longer accelerate first-passage.

at the point of resetting transition, where $r^* = 0$, as expected. Fig. 6 clearly shows that introduction of resetting with an optimal rate can even make the original first-passage process almost ten times faster!

Next, we proceed to explore the other scenario, viz., where the absorbing boundary (x_a) is placed to the left hand side of x_0 .

V. FIRST-PASSAGE FROM x_0 TO x_a : WHEN THE BOUNDARY IS PLACED CLOSER TO THE ORIGIN COMPARED TO THE INITIAL POSITION ($x_a < x_0$)

When $x_a < x_0$, the particle undergoes Feller diffusion in the interval $\Omega = [x_a, \infty)$. Note that the placement of the boundary closer to the origin compared to the initial position suggests that in this case, the first-passage is being considered from a more diffusive to a less diffusive zone. Moreover, in contrast to the previous case, studied in Section IV, now the domain Ω is *semi-infinite*. Recalling the general expression of $Q_r(s|x_0)$ given in Eq. (15), we see that in the limit $x_0 \rightarrow \infty$, $M(s+r; \theta; x_0)$ diverges. Therefore, to keep $\tilde{Q}_r(s|x_0)$ finite for all values of x_0 , we set $c_1 = 0$. The absorbing boundary at x_a then gives $c_2 = -[1 + r\tilde{Q}_r(s|x_r)] / [(s+r)U(s+r; \theta; x_a)]$. Putting these values of c_1 and c_2 in Eq. (15), we retrieve the specific solution for Eq. (13) for $x_a < x_0$, which reads

$$\tilde{Q}_r(s|x_0) = \frac{1 + r\tilde{Q}_r(s|x_r)}{s+r} \left[1 - \frac{U(s+r; \theta; x_0)}{U(s+r; \theta; x_a)} \right]. \quad (21)$$

In a similar manner as before, we set $x_r = x_0$ in Eq. (21), i.e. coincide the position of resetting with the initial position, to obtain the following expression of $\tilde{Q}_r(s|x_0)$ in a self consistent

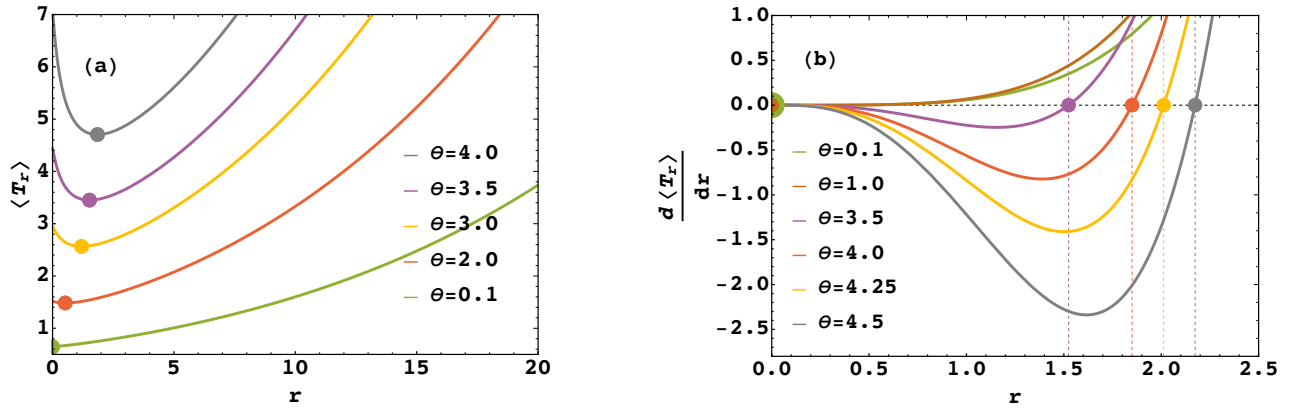


FIG. 7. First-passage with resetting for $x_a < x_0$. Panel (a): The mean FPT $\langle T_r \rangle$ vs. the resetting rate r following Eq. (23) for different values of θ , where $x_a = 1$ and $x_0 = 2.5$. $\langle T_r \rangle$ shows monotonic increase with r for lower values of θ , and the optimal resetting rates (r^*), marked by colored discs, are zero in this regime. In contrast, for higher values of θ , the variation of $\langle T_r \rangle$ with r becomes non-monotonic and r^* become non-zero. Panel (b): Graphical solution of Eq. (24) for different values of θ , where $x_a = 1$ and $x_0 = 2.5$. The solutions, denoted r^* , are marked by colored discs.

manner

$$\tilde{Q}_r(s|x_0) = \frac{1 - \frac{U(s+r; \theta; x_0)}{U(s+r; \theta; x_a)}}{s + r \left[\frac{U(s+r; \theta; x_0)}{U(s+r; \theta; x_a)} \right]}. \quad (22)$$

Note that in the absence of resetting, i.e., when $r \rightarrow 0$, Eq. (22) reduces to Eq. (7), as expected. Setting $s = 0$ in Eq. (22), we obtain the mean first-passage time

$$\langle T_r \rangle = \frac{1}{r} \left[\frac{U(r; \theta; x_a)}{U(r; \theta; x_0)} - 1 \right]. \quad (23)$$

In Fig. 7(a), we plot the mean FPT $\langle T_r \rangle$ as a function of the resetting rate, r , following Eq. (23). Fig. 7(a) shows that [in complete contrast with the previous case, where $x_0 < x_a$] for lower values of θ , $\langle T_r \rangle$ increases monotonically with r ,

which indicates that resetting can not expedite first-passage in that case. However, for higher values of θ , $\langle T_r \rangle$ show a non-monotonic variation, where the initial reduction of the mean FPT with the resetting rate indicates that resetting can successfully lower $\langle T_r \rangle$ here. Therefore, the optimal resetting rate is zero for lower values of θ and that becomes non-zero when θ increases beyond a threshold value, θ_c [not shown in Fig. 7(a)]. Next, we explore the resulting resetting transition in terms of the optimal resetting rate, i.e., the resetting rate that minimizes the mean FPT.

A. The optimal resetting rate for $x_a < x_0$

Letting r^* denote the optimal resetting rate as before, we differentiate Eq. (23) with r and equate it to zero for $r = r^*$ to obtain

$$\left[\frac{d\langle T_r \rangle}{dr} \right]_{r=r^*} = \frac{1}{(r^*)^2 U(r^*; \theta; x_0)} \left[-r^* U(r^*; \theta; x_a) \left(\frac{\partial U(r; \theta; x_0)}{\partial r} \right)_{r=r^*} + U(r^*; \theta; x_0) [U(r^*; \theta; x_0) - U(r^*; \theta; x_a) + r^* \left[\frac{\partial U(r; \theta; x_a)}{\partial r} \right]_{r=r^*}] \right] = 0 \quad (24)$$

Eq. (24) is a transcendental equation [like Eq. (19)], and hence we need to solve it numerically in order to calculate r^* . In Fig. 7(b), we plot $\left[\frac{d\langle T_r \rangle}{dr} \right]_{r=r^*}$ vs. r from Eq. (24) to graphically solve the same in a similar way as in Sec. IV. It is clear from Fig. 7(b) that the optimal resetting rates are zero for $\theta \leq \theta_c$, and resetting expedites the dynamics only when $\theta > \theta_c$, indicated by the non-zero values of r^* . We can qualitatively explain this trend by considering Feller process as space-dependent diffusion in a unique harmonic potential

$U(x) = x \left(\frac{x}{2} - \theta \right)$, as discussed earlier. For the present case, i.e., $x_a < x_0$, the relative placements of θ with x_0 and x_a can create three distinct possibilities, viz., (i) $\theta \leq x_a < x_0$, (ii) $x_a < \theta \leq x_0$ and (iii) $x_a < x_0 < \theta$. We illustrate these three cases in Fig. 8, where we plot $U(x)$ vs. x for three different values of θ . Since θ represents the equilibrium position of $U(x)$, for case (i) the first-passage is a journey downhill [marked by the green arrow above curve(i)], while it is an uphill one for case (iii) [marked by the green arrow above

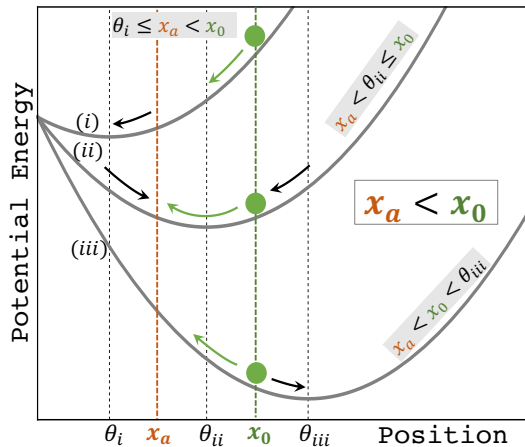


FIG. 8. Schematic plot of the potential $U(x) = x(\frac{x}{2} - \theta)$ vs. x to mark the three scenarios that arise in connection to the first-passage from x_0 to x_a for $x_0 < x_a$, shown by three $U(x)$ curves with different minima, such that $\theta_i < \theta_{ii} < \theta_{iii}$. The green arrow in each case indicate the overall direction of first-passage, whereas the black arrows indicate the drift velocity generated by $U(x)$. When these forces assist each other, resetting is expected to delay first-passage [e.g., $\theta_i \leq x_a < x_0$]. In contrast, when these forces oppose each other, resetting is expected to accelerate first-passage [e.g., $x_a < x_0 < \theta_{iii}$]. An intermediate case is observed for $x_a < \theta_{ii} \leq x_0$.

curve(iii)]. As shown in Fig. 8, the drift velocity acts towards the absorbing boundary for case (i) [marked by the black arrow above curve (i)], and thereby assists the first-passage; resetting at $x_0 > \theta$ thus interrupts the original process and delays it. In contrast, the drift velocity for case (iii) acts away from x_a [marked by the black arrow above curve (iii)], and thereby opposes the first-passage; resetting at $x_0 < \theta$ thus accelerates the process. Case (ii) represents an intermediate scenario between these two extreme cases, shown by curve (ii) in Fig. 8.

To explore the resetting transition further, next we numerically solve Eq. (24) to calculate r^* as a function of θ for different values of x_0 , keeping x_a constant. Plotting the results in Fig. 9, we observe that when x_0 is considerably small, i.e., when the distance to travel is short, resetting always expedites first-passage, which means resetting transition can even be non-existent! For higher values of x_0 , however, the transition is observed and the threshold value of θ corresponding to the transition, i.e. θ_c , increases with x_0 . To qualitatively explain this trend, we recall that Feller process can be envisioned as *space-dependent* diffusion [in a potential $U(x) = x(\frac{x}{2} - \theta)$] with a diffusion coefficient $D(x) = x$. This makes the potential *effectively* asymmetric (or ‘tilted’) around the equilibrium position θ , such that the left branch of the potential appears a lot steeper to the particle compared to the right branch. Indeed, the particle diffuses almost freely when $x \gg \theta$. Additionally, it can experience trapping around θ , but that does not affect the dynamics as significantly as in the previous case for the following reasons: (a) for smaller values of θ , the potential is shallow and hence not very effective in trapping the particle successfully and (b) for larger values of θ , though the depth of the potential increases, the trapping is counterbalanced by the

higher diffusion coefficient. Now, if the distance between the absorbing boundary and initial position is small and both are placed somewhat close to the origin, resetting at x_0 accelerates first-passage by cutting short the long trajectories that may generate as the particle diffuses far away from the origin. In contrast, when the distance between x_a and x_0 is large [and x_a is still kept close to the origin], resetting the particle in an almost free-diffusing zone far away from the boundary does not help expediting first-passage anymore unless θ is sufficiently high [see Fig. 8]. Therefore, when x_0 is increased keeping x_a unaltered, θ_c is observed to increase. Summarizing, we see that for $x_a < x_0$, resetting expedites first-passage for $\theta > \theta_c$ and θ_c increases as the distance to travel increases. Finally, we quantify the effect of optimal resetting on the dynamics, by calculating the maximal speedup, as we did earlier.

B. Maximal speedup for $x_a < x_0$

Since the maximal speedup of a first-passage process is defined as the ratio between the mean FPT for the original process (i.e., the process without resetting) to the mean FPT of the process with optimal resetting, setting $r = r^*$ in Eq. (23) and using Eq. (A.33) from Appendix A, we obtain

$$\frac{\langle T \rangle}{\langle T_{r^*} \rangle} = \frac{r^* \left(\left[\frac{\partial U(s; \theta; x_a)}{\partial s} \right]_{s \rightarrow 0} - \left[\frac{\partial U(s; \theta; x_0)}{\partial s} \right]_{s \rightarrow 0} \right)}{\frac{U(r^*; \theta; x_a)}{U(r^*; \theta; x_0)} - 1}. \quad (25)$$

Plugging in r^* [obtained earlier by numerically solving Eq. (24)] into Eq. (25), we calculate the maximal speedup of the first-passage process from x_0 to x_a , when $x_a < x_0$. Plotting Eq. (25) with respect to θ for different values of x_0 in Fig. 10, we see that the maximal speedup is most significant when θ

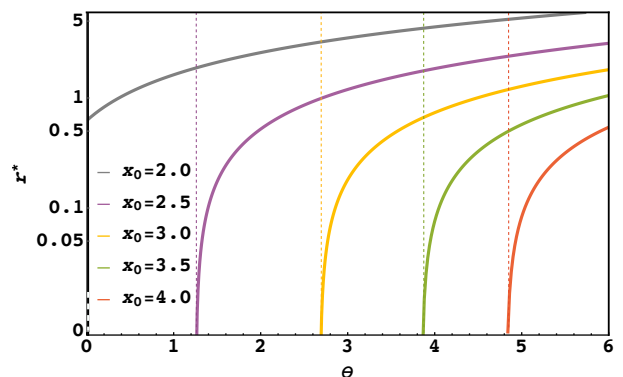


FIG. 9. The optimal resetting rate r^* , obtained from the numerical solution of Eq. (24), vs. θ for different initial positions, x_0 , when $x_a < x_0$. The non-zero values of r^* mark the regime when resetting accelerates first-passage from x_0 to x_a , observed for higher values of θ . The resetting transitions are clearly indicated by the dashed vertical lines of the same color as the curves. The position of the absorbing boundary is kept fixed at $x_a = 1$ in each case. With increase in x_0 , the transition is observed to take place at higher values of θ . When the distance to travel is short enough, resetting always expedites first-passage, as observed for $x_0 = 2.0$ (gray curve).

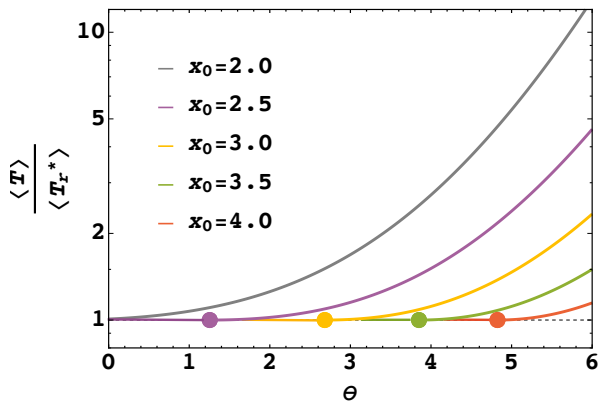


FIG. 10. Maximal speedup $\langle T \rangle / \langle T_{r^*} \rangle$ vs. θ following Eq. (25) for different values of x_0 , where $x_a < x_0$. The colors of the curves correspond to the cases shown in Fig. 9. In most cases (except for the case of $x_0 = 2$, shown by the gray curve), maximal speedup is unity for lower values of θ , which indicates that resetting does not expedite first-passage there. Most significant maximal speedup is observed for higher values of θ . The resulting resetting transition are marked by colored discs.

is large, indicating that resetting in this regime helps the most. With decrease in θ , however, the maximal speedup gradually decreases, until it becomes unity at the point of resetting transition, where r^* becomes zero. Note that for $x_0 = 2$ (shown by the grey curve in Fig. 9), the maximal speedup is *not* unity for small values of θ ; it just appears so in comparison to the significantly larger values of the maximal speedup that are observed for the higher values of θ .

VI. CONCLUSIONS

In this work, we explored the first-passage properties associated to Feller diffusion with Poissonian resetting. Considering Feller process as space-dependent diffusion with a diffusion coefficient $D(x) = x$ in a potential $U(x) = x(\frac{x}{2} - \theta)$, we calculated the first-passage time using the Fokker-Planck description of the system. Closed-form formulæ were obtained for the Laplace transform of the survival probability, which in turn generated the exact expression of the mean FPT. We calculated the optimal resetting rates (rate of resetting that minimizes the mean FPT), which manifest a hallmark of *resetting transition* depending upon the governing parameters, viz., the equilibrium position of the Feller potential (θ), the initial position of the particle executing Feller diffusion (x_0), and the position of the absorbing boundary that ensures the completion of the process (x_a). In-depth analysis were performed on the optimal resetting rate, r^* , and the maximal speedup, $\langle T \rangle / \langle T_{r^*} \rangle$, to identify the parameter space where Poissonian resetting accelerates Feller diffusion. The entire study was executed for two distinct cases: (a) when the absorbing boundary is placed further away from the origin compared to the initial position (or the starting value of the process lies below the target value, i.e., $x_0 < x_a$) and (b) when the absorbing boundary is placed closer to the origin compared to the ini-

tial position (or the starting value of the process lies above the target value, i.e., $x_a < x_0$). For the former case, resetting was found to expedite first-passage from x_0 to x_a for $\theta < \theta_c$, where θ_c is a critical value of θ , which decreases when x_a is moved away from the origin (and hence from x_0). In complete contrast, resetting was observed to expedite first-passage for $\theta > \theta_c$, where θ_c is again a threshold value of θ , which increases when x_0 is moved away from the origin (and hence from x_a). Interestingly enough, our study indicates that irrespective of that placement of the target value (x_a) either above or below the initial value (x_0) of the Feller process, the volume of the phase space where resetting expedites first-passage is always smaller when the distance to travel is large, which is evident from Fig. 4 and Fig. 9. Since Feller process with resetting finds direct applications in various fields ranging from population dynamics to financial markets, we hope that the present work will attract attention from multiple disciplines associated to biological and social sciences.

DATA AVAILABILITY

The data supporting this study are available within the article and its appendix.

ACKNOWLEDGEMENTS

The author acknowledges the INSPIRE Faculty fellowship and research grant (IFA19-CH326) from the Department of Science & Technology, Govt. of India, executed at IIT Tirupati through Project No. CHY/2021/005/DSTX/SOMR. Sincere thanks are due to MPIPKS, Dresden, Germany for hospitality during Summer, 2022.

APPENDIX A: DERIVATION OF $CV(T)$, THE COEFFICIENT OF VARIATION OF FIRST-PASSAGE TIME FOR FELLER DIFFUSION WITHOUT RESETTING

The coefficient of variation of the FPT is defined as the ratio of the standard deviation in the first-passage time T to its mean, i.e., $CV(T) := \sigma(T) / \langle T \rangle$, where $\sigma(T) := [\langle T^2 \rangle - \langle T \rangle^2]^{1/2}$ is the standard deviation in T . Therefore, to calculate $CV(T)$, we need to calculate $\langle T \rangle$ and $\langle T^2 \rangle$, i.e., the first and second moment of the FPT distribution. These two observables can be calculated from the survival probability of the associated first-passage process. Here we derive approximate expressions of $CV(T)$ for the two different boundary conditions that are discussed in the main text, starting with $x_0 < x_a$.

The mean first-passage time is related to the survival probability in the Laplace space as $\langle T \rangle = [\tilde{Q}(s|x_0)]_{s \rightarrow 0}$. Expanding $M(s; \theta; x_i)$ [defined in Eq. (6)] in Taylor series around $s = 0$,

for small values of s we can write

$$M(s; \theta; x_i) \sim 1 + \left[\frac{\partial M(s; \theta; x_i)}{\partial s} \right]_{s \rightarrow 0} s + \frac{1}{2} \left[\frac{\partial^2 M(s; \theta; x_i)}{\partial s^2} \right]_{s \rightarrow 0} s^2 \quad (\text{A.26})$$

where $i \equiv 0, a$. Plugging in that into Eq. (5) we get

$$\tilde{Q}(s|x_0) \sim \frac{1}{s} \left[1 - \frac{1 + \left[\frac{\partial M(s; \theta; x_0)}{\partial s} \right]_{s \rightarrow 0} s + \frac{1}{2} \left[\frac{\partial^2 M(s; \theta; x_0)}{\partial s^2} \right]_{s \rightarrow 0} s^2}{1 + \left[\frac{\partial M(s; \theta; x_a)}{\partial s} \right]_{s \rightarrow 0} s + \frac{1}{2} \left[\frac{\partial^2 M(s; \theta; x_a)}{\partial s^2} \right]_{s \rightarrow 0} s^2} \right]. \quad (\text{A.27})$$

In the limit $s \rightarrow 0$, Eq. (A.27) gives an approximate expression for the mean FPT of Feller diffusion for $x_0 < x_a$, which reads

$$\langle T \rangle = \left[\frac{\partial M(s; \theta; x_a)}{\partial s} \right]_{s \rightarrow 0} - \left[\frac{\partial M(s; \theta; x_0)}{\partial s} \right]_{s \rightarrow 0} \quad (\text{A.28})$$

Since $\langle T^2 \rangle = -2 \left[\frac{d\tilde{Q}(s|x_0)}{ds} \right]_{s \rightarrow 0}$, differentiating Eq. (A.27) with respect to s and setting the limit $s \rightarrow 0$, we obtain

$$\langle T^2 \rangle = 2 \left[\left[\frac{\partial M(s; \theta; x_a)}{\partial s} \right]_{s \rightarrow 0} - \left[\frac{\partial M(s; \theta; x_0)}{\partial s} \right]_{s \rightarrow 0} \right] \left[\frac{\partial M(s; \theta; x_a)}{\partial s} \right]_{s \rightarrow 0} + \left[\frac{\partial^2 M(s; \theta; x_0)}{\partial s^2} \right]_{s \rightarrow 0} - \left[\frac{\partial^2 M(s; \theta; x_a)}{\partial s^2} \right]_{s \rightarrow 0}. \quad (\text{A.29})$$

Utilizing Eq. (A.28) and Eq. (A.29), we obtain an expression for $CV(T)$ that reads

$$CV(T) = \frac{\sqrt{\left[\frac{\partial^2 M(s; \theta; x_0)}{\partial s^2} \right]_{s \rightarrow 0} - \left[\frac{\partial^2 M(s; \theta; x_a)}{\partial s^2} \right]_{s \rightarrow 0} + \left(\left[\frac{\partial M(s; \theta; x_a)}{\partial s} \right]_{s \rightarrow 0} \right)^2 - \left(\left[\frac{\partial M(s; \theta; x_0)}{\partial s} \right]_{s \rightarrow 0} \right)^2}}{\left[\frac{\partial M(s; \theta; x_a)}{\partial s} \right]_{s \rightarrow 0} - \left[\frac{\partial M(s; \theta; x_0)}{\partial s} \right]_{s \rightarrow 0}} \quad \text{for } x_0 < x_a. \quad (\text{A.30})$$

We calculate $CV(T)$ following Eq. (A.30) and plot that in Fig. 2(a) in the main text.

In a similar manner, for $x_a < x_0$, we can expand $U(s; \theta; x_i)$ [defined in Eq. (8)] in Taylor series around $s = 0$ and for small values of s that reads

$$U(s; \theta; x_i) \sim 1 + \left[\frac{\partial U(s; \theta; x_i)}{\partial s} \right]_{s \rightarrow 0} s + \frac{1}{2} \left[\frac{\partial^2 U(s; \theta; x_i)}{\partial s^2} \right]_{s \rightarrow 0} s^2, \quad (\text{A.31})$$

for $i \equiv 0, a$. Plugging in the expression of $U(s; \theta; x_i)$ from Eq. (A.31) into Eq. (7), we obtain

$$\tilde{Q}(s|x_0) \sim \frac{1}{s} \left[1 - \frac{1 + \left[\frac{\partial U(s; \theta; x_0)}{\partial s} \right]_{s \rightarrow 0} s + \frac{1}{2} \left[\frac{\partial^2 U(s; \theta; x_0)}{\partial s^2} \right]_{s \rightarrow 0} s^2}{1 + \left[\frac{\partial U(s; \theta; x_a)}{\partial s} \right]_{s \rightarrow 0} s + \frac{1}{2} \left[\frac{\partial^2 U(s; \theta; x_a)}{\partial s^2} \right]_{s \rightarrow 0} s^2} \right],$$

$$\quad (\text{A.32})$$

which the limit of $s \rightarrow 0$ gives

$$\langle T \rangle = \left[\frac{\partial U(s; \theta; x_a)}{\partial s} \right]_{s \rightarrow 0} - \left[\frac{\partial U(s; \theta; x_0)}{\partial s} \right]_{s \rightarrow 0}. \quad (\text{A.33})$$

Differentiating Eq. (A.32) with respect to s , in the limit $s \rightarrow 0$ we obtain

$$\langle T^2 \rangle = 2 \left[\left[\frac{\partial U(s; \theta; x_a)}{\partial s} \right]_{s \rightarrow 0} - \left[\frac{\partial U(s; \theta; x_0)}{\partial s} \right]_{s \rightarrow 0} \right] \left[\frac{\partial U(s; \theta; x_a)}{\partial s} \right]_{s \rightarrow 0} + \left[\frac{\partial^2 U(s; \theta; x_0)}{\partial s^2} \right]_{s \rightarrow 0} - \left[\frac{\partial^2 U(s; \theta; x_a)}{\partial s^2} \right]_{s \rightarrow 0}. \quad (\text{A.34})$$

From Eq. (A.33) and Eq. (A.34), we finally get

$$CV(T) = \frac{\sqrt{\left[\frac{\partial^2 U(s; \theta; x_0)}{\partial s^2} \right]_{s \rightarrow 0} - \left[\frac{\partial^2 U(s; \theta; x_a)}{\partial s^2} \right]_{s \rightarrow 0} + \left(\left[\frac{\partial U(s; \theta; x_a)}{\partial s} \right]_{s \rightarrow 0} \right)^2 - \left(\left[\frac{\partial U(s; \theta; x_0)}{\partial s} \right]_{s \rightarrow 0} \right)^2}}{\left[\frac{\partial U(s; \theta; x_a)}{\partial s} \right]_{s \rightarrow 0} - \left[\frac{\partial U(s; \theta; x_0)}{\partial s} \right]_{s \rightarrow 0}} \quad \text{for } x_a < x_0. \quad (\text{A.35})$$

We calculate $CV(T)$ for $x_a < x_0$ from Eq. (A.35) and plot the

same in Fig. 2(b) in the main text.

- [1] W. Feller, *Two singular diffusion problems*, *Ann. Math.* **54**, 173 (1951).
- [2] W. Feller, *The Parabolic Differential Equations and the Associated Semi-Groups of Transformations*, *Ann. Math.* **55**, 468 (1952).
- [3] W. Feller, *Diffusion processes in one dimension*, *Trans. Amer. Math. Soc.* **77**, 1 (1954).
- [4] J. Masoliver and J. Perelló, *First-passage and escape problems in the Feller process*, *Phys. Rev. E* **86**, 041116, (2012).
- [5] A. J. Lotka, *Elements of Physical Biology*, Williams and Wilkins, (1925).
- [6] V. Volterra, *Variations and fluctuations of the number of individuals in animal species living together in Animal Ecology*, McGraw-Hill, (1931).
- [7] R. M. Capocelli and L. M. Ricciardi, *A diffusion model for population growth in random environment*, *Theoretical Population Biology* **5**, 28, (1974).
- [8] R. M. Capocelli and L. M. Ricciardi, *Growth with Regulation in Random Environment*, *Kybernetik* **15**, 147, (1974).
- [9] S. Azaele, A. Maritan, E. Bertuzzo, I. Rodriguez-Iturbe, and A. Rinaldo, *Stochastic dynamics of cholera epidemics*, *Phys. Rev. E* **81**, 051901, (2010).
- [10] S. Redner, *A guide to first-passage processes*, Cambridge University Press, (2001).
- [11] *A continuous markovian model for neuronal activity*, *J. theor. Biol.* **40**, 369, (1973).
- [12] T. Tchumatchenko, A. Malyshev, T. Geisel, M. Volgushev, and F. Wolf, *Correlations and Synchrony in Threshold Neuron Models*, *Phys. Rev. Lett.* **104**, 058102, (2010).
- [13] S. Ditlevsen and P. Lansky *Estimation of the input parameters in the Feller neuronal model*, *Phys. Rev. E* **73**, 061910, (2006).
- [14] P. Lansky and S. Ditlevsen *A review of the methods for signal estimation in stochastic diffusion leaky integrate-and-fire neuronal models*, *Biol. Cybern.* **99**, 253, (2008).
- [15] E. Bibbona, P. Lansky, and Roberta Sirovich *Estimating input parameters from intracellular recordings in the Feller neuronal model*, *Phys. Rev. E* **81**, 031916, (2010).
- [16] G. D'Onofrio, P. Lansky, and E. Pirozzi, *On two diffusion neuronal models with multiplicative noise: The mean first-passage time properties*, *Chaos* **28**, 043103, (2018).
- [17] J. C. Cox, J. E. Ingersoll, and S. A. Ross, *A Theory of the Term Structure of Interest Rates*, *Econometrica* **53**, 385, (1985).
- [18] S. L. Heston, *A Closed-Form Solution for Options with Stochastic Volatility with Applications to Bond and Currency Options*, *Rev. Financ. Stud.* **6**, 327, (1993).
- [19] A. A. Dragulescu and V. M. Yakovenko, *Probability distribution of returns in the Heston model with stochastic volatility*, *Quant. Fin.* **2**, 443, (2002).
- [20] P. Richmond and L. Sabatelli, *Langevin processes, agent models and socio-economic systems*, *Physica A* **336**, 27, (2004).
- [21] R. F. Engle and A. J. Patton *What good is a volatility model?*, *Quant. Fin.* **1**, 237, (2001).
- [22] P. Visco, R. J. Allen, S. N. Majumdar, and M. R. Evans, *Switching and growth for microbial populations in catastrophic responsive environments*, *Biophys. J.* **98**, 1099 (2010).
- [23] D. Sornette, *Critical market crashes*, *Phys. Rep.* **378**, 1, (2003).
- [24] M. R. Evans, S. N. Majumdar, and G. Schehr, *Stochastic resetting and applications*, *J. Phys. A: Math. Theor.* **53**, 193001, (2020).
- [25] M. R. Evans, and S. N. Majumdar, *Diffusion with stochastic resetting*, *Phys. Rev. Lett.* **106**, 160601 (2011).
- [26] M. R. Evans, and S. N. Majumdar, *Diffusion with optimal resetting*, *J. Physics A: Math. Theor.* **44**, 435001 (2011).
- [27] M. R. Evans, and S. N. Majumdar, *Diffusion with resetting in arbitrary spatial dimension*, *J. Physics A: Math. Theor.* **47**, 285001 (2014).
- [28] S. Reuveni, M. Urbakh, and J. Klafter, *Role of substrate unbinding in Michaelis–Menten enzymatic reactions*, *Proc. Natl. Acad. Sci. U. S. A.* **111**, 4391 (2014).
- [29] S. Reuveni, *Optimal stochastic restart renders fluctuations in first passage times universal*, *Phys. Rev. Lett.* **116**, 170601 (2016).
- [30] S. Ray, D. Mondal, and S. Reuveni, *Péclet number governs transition to acceleratory restart in drift-diffusion*, *J. Phys. A: Math. Theor.* **52**, 255002 (2019).
- [31] S. Ahmad, I. Nayak, A. Bansal, A. Nandi, and D. Das, *First passage of a particle in a potential under stochastic resetting: a vanishing transition of optimal resetting rate*, *Phys. Rev. E* **99**, 022130 (2019).
- [32] A. Pal and V. V. Prasad, *Landau theory of restart transitions*, *Phys. Rev. Research* **1**, 032001 (2019).
- [33] S. Ray and S. Reuveni, *Diffusion with resetting in a logarithmic potential*, *J. Chem. Phys.* **152**, 234110 (2020).
- [34] S. Ray, *Space-dependent diffusion with stochastic resetting: A first-passage study*, *J. Chem. Phys.* **153**, 234904 (2020).
- [35] S. Ray and S. Reuveni, *Resetting transition is governed by an interplay between thermal and potential energy*, *J. Chem. Phys.* **154**, 171103 (2021).
- [36] Ł. Kuśmierz, S. N. Majumdar, S. Sabhapandit, and G. Schehr, *First order transition for the optimal search time of Lévy flights with resetting*, *Phys. Rev. Lett.* **113**, 220602, (2014).
- [37] D. Campos, and V. Méndez, *Phase transitions in optimal search times: How random walkers should combine resetting and flight scales*, *Phys. Rev. E* **92**, 062115, (2015).
- [38] É. Roldán, A. Lisica, D. Sánchez-Taltavull, and S. W. Grill, *Stochastic resetting in backtrack recovery by RNA polymerases*, *Phys. Rev. E* **93**, 062411 (2016).
- [39] A. Pal, A. Kundu, and M. R. Evans, *Diffusion under time-dependent resetting*, *J. Physics A: Math. Theor.* **49**, 225001 (2016).
- [40] U. Bhat, C. De Bacco, and S. Redner, *Stochastic search with Poisson and deterministic resetting*, *J. Stat. Mech.* **2016**, 083401, (2016).
- [41] A. Pal, and S. Reuveni, *First Passage under Restart*, *Phys. Rev. Lett.* **118**, 030603, (2017).
- [42] S. Belan, *Restart could optimize the probability of success in a Bernoulli trial*, *Phys. Rev. Lett.* **120**, 080601, (2018).
- [43] M. R. Evans, and S. N. Majumdar, *Effects of refractory period on stochastic resetting*, *J. Phys. A: Math. Theor.* **52**, 01LT01, (2018).
- [44] A. Pal, Ł. Kuśmierz, and S. Reuveni, *Search with home returns provides advantage under high uncertainty*, *Phys. Rev. Research*, **2**, 043174, (2019).
- [45] C. A. Plata, D. Gupta, and S. Azaele, *Asymmetric stochastic resetting: Modeling catastrophic events*, *Phys. Rev. E*, **102**, 052116, (2020).
- [46] G. Tucci, A. Gambassi, S. Gupta, and É. Roldán, *Controlling particle currents with evaporation and resetting from an interval*, *Phys. Rev. Research* **2**, 043138 (2020).
- [47] A. Pal, S. Kostinski, and S. Reuveni, *The inspection paradox in stochastic resetting*, *J. Phys. A: Math. Theor.* **55**, 021001, (2022).

- [48] T. Sandev, V. Domazetoski, L. Kocarev, R. Metzler and A. Chechkin, *Heterogeneous diffusion with stochastic resetting*, *J. Phys. A: Math. Theor.* **55**, 074003, (2022).
- [49] S. Y. Ali, N. Choudhury, and D. Mondal *Asymmetric restart in a stochastic climate model: A theoretical perspective to prevent the abnormal precipitation accumulation caused by global warming*, *J. Phys. A: Math. Theor.*, **55**, 301001 (2022).
- [50] O. Tal-Friedman, A. Pal, A. Sekhon, S. Reuveni, and Y. Roichman, *Experimental realization of diffusion with stochastic resetting*, *J. Phys. Chem. Lett.*, **11**, 7350, (2020).
- [51] B. Besga, A. Bovon, A. Petrosyan, S. N. Majumdar, and S. Ciliberto, *Optimal mean first-passage time for a Brownian searcher subjected to resetting: Experimental and theoretical results*, *Phys. Rev. Research*, **2** 032029(R) (2020).
- [52] H. Risken, *The Fokker-Planck Equation: Method of Solution and Applications*, Springer-Verlag Berlin Heidelberg New York Tokyo, (1984).
- [53] C. W. Gardiner, *Handbook of Stochastic Methods for Physics, Chemistry and the Natural Sciences*, Springer-Verlag., (2003).
- [54] Digital Library of Mathematical Functions, National Institute of Standards and Technology (NIST), U.S. Department of Commerce, <https://dlmf.nist.gov/>.
- [55] G. B. Arfken, H. J. Weber, and F. E. Harris, *Mathematical Methods for Physicists: A Comprehensive Guide*, Elsevier, Seventh Edition, (2013).
- [56] W. Magnus, H. Oberhettinger, and R. P. Soni, *Formulas and Theorems for the Special Functions of Mathematical Physics*, Springer-Verlag Berlin Heidelberg GmbH, Third Edition, (1966).